

1 Extracellular Electron Uptake by Two *Methanosarcina* Species

2 Authors:

3 Mon Oo Yee¹, Oona Snoeyenbos-West^{1,2,a}, Bo Thamdrup¹, Lars DM Ottosen², Amelia-Elena Rotaru^{1*}

4 ¹ Nordcee, Department of Biology, University of Southern Denmark, Odense, Denmark

5 ² Department of Engineering, University of Aarhus, Aarhus, Denmark

6 ^a (Current address) Department of Microbiology & Molecular Genetics, Michigan State University, East
7 Lansing, USA

8 *Correspondence to: arotaru@biology.sdu.dk

9 Abstract

10 Direct electron uptake by prokaryotes is a recently described mechanism with a potential application for
11 energy and CO₂ storage into value added chemicals. Members of Methanosarcinales, an
12 environmentally and biotechnologically relevant group of methanogens, were previously shown to
13 retrieve electrons from an extracellular electrogenic partner performing Direct Interspecies Electron
14 Transfer (DIET) and were therefore proposed to be electroactive. However, their intrinsic
15 electroactivity has never been examined. In this study, we tested two methanogens belonging to the
16 genus *Methanosarcina*, *M. barkeri* and *M. horonobensis*, regarding their ability to accept electrons
17 directly from insoluble electron donors like other cells, conductive particles and electrodes. Both
18 methanogens were able to retrieve electrons from *Geobacter metallireducens* via DIET. Furthermore,
19 DIET was also stimulated upon addition of electrically conductive granular activated carbon (GAC)
20 when each was co-cultured with *G. metallireducens*. However, when provided with a cathode poised at
21 -400 mV (vs. SHE), only *M. barkeri* could perform electromethanogenesis. In contrast, the strict
22 hydrogenotrophic methanogen, *Methanobacterium formicicum*, did not produce methane regardless of
23 the type of insoluble electron donor provided (*Geobacter* cells, GAC or electrodes). A comparison of
24 functional gene categories between the two *Methanosarcina* showed differences regarding energy

25 metabolism, which could explain dissimilarities concerning electromethanogenesis at fixed potentials.
26 We suggest that these dissimilarities are minimized in the presence of an electrogenic DIET partner
27 (e.g. *Geobacter*), which can modulate its surface redox potentials by adjusting the expression of
28 electroactive surface proteins.

29 **Introduction**

30 Extracellular electron uptake by methanogens may impact carbon turnover in electron-acceptor limited
31 environments (Morris et al., 2013). In these environments, thermodynamically challenging processes
32 become possible due to syntrophic interactions between bacteria and archaea. A syntrophic interaction
33 requires a bacterium, which oxidizes organics to interspecies-transferable molecules. Moreover,
34 syntrophy requires a partner methanogen to scavenge the transferable molecules. For decades, we have
35 assumed that interspecies-transferable molecules were either H₂ or formate (Stams and Plugge, 2009).
36 We now know that some species can also transfer electrons directly (Lovley, 2017). During direct
37 interspecies electron transfer (DIET), species like *Geobacter* oxidize ethanol according to reaction (1),
38 only in the presence of methanogens like *Methanosarcina*, which scavenge reducing equivalents (H⁺
39 and e⁻) and acetate (Rotaru et al., 2014a, 2014b) (**Fig. 1**).



43 In DIET co-cultures, only those *Geobacter* species producing high current densities, met the energetic
44 needs of their DIET partners (Rotaru et al., 2015). For this purpose, *Geobacter* up-regulates the
45 expression of redox active and conductive proteins (outer membrane *c*-type cytochromes and pili)
46 (Holmes et al., 2018b; Shrestha et al., 2013). *Geobacter*'s requirement for outer-surface proteins during
47 DIET was confirmed earlier with gene-deletion studies (Rotaru et al., 2014a, 2014b). Thus, if
48 *Geobacter* lacked the ability to produce e.g. pili it was incapable of DIET.

49 Although we understand how *Geobacter* releases electrons outside their cells during DIET, the way
50 *Methanosarcinales* retrieve DIET-electrons is poorly understood. A glimpse at this mechanism was

51 provided in a recent comparative transcriptomic study (Holmes et al., 2018b). In this study, the
52 transcriptomes of DIET co-cultures (*G. metallireducens* – *Methanosarcina barkeri*) were compared to
53 those of co-cultures performing interspecies H₂-transfer (*Pelobacter carbinolicus* – *M. barkeri*). During
54 DIET, *M. barkeri* had higher expression of membrane-bound redox-active proteins like cupredoxins,
55 thioredoxins, pyrroloquinoline, and quinone-, cytochrome- or Fe-S containing proteins (Holmes et al.,
56 2018b). Still, the exact mechanism of electron uptake by *Methanosarcina* has not been validated and
57 warrants further investigation.

58 Moreover, *Methanosarcina* can also retrieve electrons from electrically conductive particles charged by
59 *Geobacter* oxidizing organics (Shrestha and Rotaru, 2014). In effect, DIET is accelerated by electrically
60 conductive particles/minerals perhaps because they replace conductive and redox active surface proteins
61 diminishing cellular energy expenditure required to overexpress such surface constituents (Liu et al.,
62 2012). For instance, co-cultures of *G. metallireducens* and *M. barkeri* were stimulated at the addition of
63 conductive particles, such as GAC (Liu et al., 2012), carbon cloth (Chen et al., 2014a), biochar (Chen et
64 al., 2014b), or magnetite (Wang et al., 2018). On the other hand, the addition of non-conductive
65 materials did not stimulate DIET (Chen et al., 2014a; Rotaru et al., 2018a). In addition, conductive
66 particles appear to play a significant role in interspecies interactions from natural and artificial
67 ecosystems such as sediments, soils, rice paddies or anaerobic digesters (Holmes et al., 2017a; Rotaru et
68 al., 2018b; Ye et al., 2018; Zhang et al., 2018). In these cases, the addition of conductive particles
69 enriched for DIET-related Methanosarcinales (Dang et al., 2016; Holmes et al., 2017b; Rotaru et al.,
70 2018a; Zheng et al., 2015). However, exceptions were observed since occasionally conductive particles
71 enriched for H₂-utilizing methanogens of the genus *Methanospirillum* (Lee et al., 2016) or
72 *Methanobacterium* (Lin et al., 2017; Zhuang et al., 2015).

73 Since methanogens retrieve extracellular electrons from cells or conductive particles to reduce CO₂ to
74 methane, it was expected that they could also retrieve electrons from a poised electrode via
75 electromethanogenesis. Nevertheless, electromethanogenesis was only verified with H₂-utilizing
76 methanogens like *Methanobacterium palustre* (Cheng et al., 2009). Yet, H₂-utilizers were incapable of
77 DIET (Rotaru et al., 2014b). Conversely, it is unknown if Methanosarcinales, which are capable of
78 DIET, are also capable of electron uptake from a cathode. Our objective was to investigate the ability to
79 carry electromethanogenesis and DIET in two *Methanosarcina* species. We have shown that both

80 *Methanosarcina* species grew by DIET, however only *M. barkeri* grew on the cathode at - 400 mV vs.
81 SHE. This indicates that extracellular electron-uptake routes from cathodes or other cells might differ
82 between *Methanosarcina* species.

83

84 **Materials and Methods**

85 **Microorganism strains and cultivation conditions**

86 *Methanosarcina barkeri* MS (DSM 800) and *Methanosarcina horonobensis* HB-1 (DSM 21571) were
87 purchased from the German culture collection DSMZ while *Methanobacterium formicicum* (NBRC
88 100475) was from the Japanese culture collection NBRC. *Geobacter metallireducens* GS-15 was sent to
89 us by Dr. Sabrina Beckmann from the University of New South Wales, Australia.

90 Routine cultivation was performed under strictly anaerobic conditions in serum bottles sealed with butyl
91 rubber stoppers and incubated statically at 37°C. All the microorganisms had been adapted to grow in
92 DSMZ medium 120c with the following modifications: 1 g/L NaCl, 0.5g/L yeast, and no tryptone
93 (Rotaru et al., 2014a). During incubations in co-cultures or for electrochemical experiments, sulfide and
94 yeast extract was omitted. When grown in pure cultures, *Methanosarcina* species were provided with 30
95 mM acetate and 20 mM methanol as methanogenic substrates, while *M. formicicum* was provided with
96 150 kPa of H₂: CO₂ (80:20) in the headspace. *G. metallireducens* was routinely grown with 20 mM
97 ethanol and 56 mM ferric citrate. All media and cultures were prepared and kept under an N₂: CO₂
98 (80:20) atmosphere.

99 The co-cultures of *Geobacter* and methanogens were initiated with 0.5 mL of *G. metallireducens* and 1
100 mL of acetate-grown *Methanosarcina*-species or H₂-grown *M. formicicum* inoculated into 8.5 ml of the
101 media prepared as above. The starting cell numbers for the methanogens in co-cultures were
102 approximately 2.6 x 10⁶ cells/mL, 8.2 x 10⁶ cells/mL and 6.7 x 10⁵ cells/mL for *M. barkeri*, *M.*
103 *formicicum* and *M. horonobensis*, respectively. The starting cell numbers for *G. metallireducens* in co-
104 cultures were circa 1.5 x 10⁵. Incubations were carried out in 20 ml pressure vials. For the co-cultures
105 ethanol (10 mM) was added as an electron donor and CO₂ was the sole electron acceptor. When noted,

106 sterile granular activated carbon (GAC) was added at a concentration of 25 g/L and prepared as
107 described before (Rotaru et al., 2018a).

108 **Electrochemical setup and measurements**

109 All bioelectrochemical incubations were carried with a modified DSMZ 120c medium (see above) in
110 the absence of sulfide and yeast extract. The pH of this medium in the bioelectrochemical reactors was
111 set to 6.5. We used bioelectrochemical reactors with a standard dual chamber configuration as shown in
112 **Figure S1**. Two-chamber glass bottles were purchased from Adams & Chittenden Scientific Glass
113 (USA) with side ports fitted with butyl septa to allow for medium transfer, sampling, and the
114 introduction of a reference electrode. Each chamber of the reactors had a total volume of 650 ml with a
115 flange diameter of 40 mm and the chambers were separated by a Nafion™ N117 proton exchange
116 membrane (Ion Power) held by an O-ring seal with a knuckle clamp.

117 Both the working and counter electrodes were made of graphite (Mersen MI Corp., Greenville USA)
118 with dimensions of 2.5 cm x 7.5 cm x 1.2 cm thus a total projected surface area of 61.5 cm². The
119 working and counter electrodes were coupled to titanium wires, which pierced through rubber stoppers
120 fitted into the main opening of each chamber. A 2 cm deep and 2 mm wide hole was drilled on the short
121 side of the electrode and a 12.5 cm long; 2 mm wide titanium rod (Alfa-Aesar, DE) was inserted and
122 sealed from the outside with biocompatible non-conductive epoxy. Electrodes with a resistance of less
123 than 10 Ω were used to ensure proper electrical connections. The assembled electrodes were introduced
124 into the chamber via the main opening and 2 mm-wide holes were drilled in the black rubber stopper to
125 allow access of the titanium rod. After autoclaving the reactors, sterile medium was transferred into the
126 reactors anaerobically and aseptically. Sterile (bleach and ethanol series) reference electrodes were
127 lodged through a side port in the working electrode chamber at a distance of about 1 cm from the
128 surface of the working electrode. After lodging the electrodes, degassing with N₂: CO₂ (80:20) for circa
129 30 minutes in each reactor chamber ensured anaerobic conditions. When the pre-cultures were in mid-
130 exponential phase, they were inoculated (20%) into fresh medium in the cathodic chamber following
131 sterile anoxic techniques to a final volume of 550 ml leaving a headspace of approximately 100 mL in
132 each chamber. The approximate cell numbers at the time of inoculation into the electrochemical
133 reactors for *M. barkeri*, *M. formicicum* and *M. horonobensis* were 2.6 x 10⁷ cells/mL, 8.2 x 10⁷ cells/mL

134 and 6.7×10^6 cells/mL respectively. Cell counts were done with microscopic examination using DAPI
135 (1 $\mu\text{g/mL}$) stained cells.

136 The reference electrodes used were leak-free Ag/AgCl reference electrodes (3.4M KCl) (CMA
137 Microdialysis, Sweden), which are 242 mV above the standard hydrogen electrode (SHE) according to
138 the manufacturer and our own measurements against a Hydroflex[®] reference electrode used as NHE
139 (normal hydrogen electrode). The difference between NHE and SHE is experimentally negligible
140 (Smith and Stevenson, 2007). All potentials in this paper from here onwards are reported vs. SHE by
141 adjusting accordingly from the Ag/AgCl reference electrodes values. Cathode poisoning and
142 electrochemical measurements were carried with a multichannel potentiostat (MultiEmstat, Palmsens,
143 NL) operated by the Multitrace software (Palmsens, NL).

144 **Analytical measurements and calculations**

145 Headspace samples for CH₄ and H₂ analysis were taken with hypodermic needles and kept in airtight
146 exetainers until measurement. Methane (CH₄) and hydrogen gas (H₂) were measured on a Trace 1300
147 gas chromatograph (Thermo-Scientific) with a TracePLOT[™] TG-BOND Msieve 5A column and a
148 thermal conductivity detector (TCD). The carrier gas was argon at a flow rate of 25 mL/min. The
149 injector, oven and detector temperatures were 150°C, 70°C, and 200°C respectively. The detection limit
150 for CH₄ and H₂ was ca. 5 μM for both. The concentration unit was converted to molarity by using the
151 ideal gas law ($p \times V = n \times R \times T$) under standard conditions, where $p = 1 \text{ atm}$, V is the volume of the
152 gaseous phase (L), n is amount of gas (mol), R is the gas constant ($0.08205 \text{ atm} \times \text{L} / \text{mol} \times \text{K}$) and $T =$
153 298.15 K. For ethanol detection, 0.5 mL samples were filtered (0.2 μm pore size) into appropriate
154 sampling vials and were heated for 5 min. at 60°C. The headspace gas was then pass through the Trace
155 1300 gas chromatograph (Thermo-Scientific) with a TRACE[™] TR-Wax column and detected by a
156 flame ionization detector (FID). Nitrogen gas at a flow of 1 mL/min was used as the carrier and the
157 injector, oven, and detectors were kept at 220°C, 40°C and 230°C respectively. Short-chained volatile
158 fatty acids (VFA) were analyzed with a Dionex[™] ICS-1500 Ion Chromatography system, using a
159 Dionex[™] IonPac[™] AS22 IC Column and a mixture of 1.4 mM NaHCO₃ and 4.5 mM Na₂CO₃ as the
160 eluent fitted with an electron capture detector (ECD) at 30 mA.

161

162 **Genome comparison**

163 Genomes for all tested microorganisms were available at the JGI integrated microbial genomes and
164 microbiomes. Functional category comparisons and pairwise average nucleotide identity (ANI) were
165 determined using the IMG/M- “Compare Genomes” tools. The IMG genome IDs of the studied *M.*
166 *barkeri*, *M. horonobensis* and *M. formicicum* used were 2630968729, 2627854269 and 2645727909
167 respectively. The gene functions were analyzed from the annotated names of all the protein-coding
168 genes retrieved from the National Center for Biotechnology Information (NCBI) database. The
169 accession numbers used were NZ_CP009528, NZ_CP009516, and NZ_LN515531 for *M. barkeri*, *M.*
170 *horonobensis* and *M. formicicum* respectively. To scan for the cytochrome motif (CxxCH) through all
171 the genomes, we used a pattern-matching Web-application (Seiler et al., 2006) in addition to manual
172 search

173 **Results and Discussion**

174 It was previously shown that two Methanosarcinales-methanogens, *Methanosarcina barkeri* and
175 *Methanotherix harundinacea* grew via DIET whereas strict H₂-utilizing methanogens did not (Rotaru et
176 al., 2014a, 2014b). Here we show that indeed *M. barkeri* could retrieve electrons not only from an
177 exoelectrogen but also from an electrode poised at - 400 mV (non-H₂ generating conditions) to carry
178 electromethanogenesis. As expected, the H₂-utilizing methanogen *M. formicicum* did not carry
179 electromethanogenesis under this condition. We tested an environmentally relevant *Methanosarcina*, *M.*
180 *horonobensis* for extracellular electron uptake from cells and electrodes, and we observed that it could
181 only retrieve electrons from exoelectrogenic *Geobacter* and from granular activated carbon but not from
182 electrodes.

183 ***Methanosarcina barkeri***

184 *M. barkeri* grows in co-culture with *G. metallireducens* via DIET, and the interaction could be
185 accelerated by electrically conductive particles (Rotaru et al., 2014a, **Fig. S2**). This was anticipated
186 because *G. metallireducens*, a respiratory organism, is incapable of substrate fermentation and
187 consequent H₂ production according to previous physiological tests (Cord-Ruwisch et al., 1998) and
188 genetic investigations (Aklujkar et al., 2009). Since H₂ could not be generated by *G. metallireducens*, a
189 strict H₂-utilizer like *M. formicicum* was rendered incapable of an interspecies association based on H₂-

190 transfer with this bacterium (Rotaru 2014b). However, more recent studies indicated that conductive
191 carbon nanotubes stimulated methanogenesis by *M. formicicum* (Salvador et al., 2017). This implied
192 that *M. formicicum* might be encouraged by the presence of conductive particle to interact
193 syntrophically with *Geobacter*. Therefore, we tested if conductive GAC aids *M. formicicum* to establish
194 a syntrophic association with *G. metallireducens*. This was not the case since co-cultures of *M.*
195 *formicicum* and *G. metallireducens* did not generate methane regardless of the presence or absence of
196 conductive particles, over the course of 120 days (**Fig. 2**).

197 During DIET, the extracellular electron transfer machinery of *G. metallireducens* plays a crucial role in
198 *Geobacter-Methanosarcina* interactions, indicating that *Geobacter* releases extracellular electrons for
199 the methanogen to use. Therefore, we suspected that *Methanosarcina* might also be able to directly
200 retrieve extracellular electrons from electrodes to do electromethanogenesis.

201 In this study, we tested for the first time if *M. barkeri* could retrieve electrons directly from an electrode
202 poised at -400 mV. Indeed, *M. barkeri* produced significantly more methane (4.4 ± 0.33 mM; $p < 0.001$)
203 (**Fig. 3**) when provided with an applied potential at the cathode, in contrast to open circuit controls
204 without an applied potential (1.3 ± 0.33 mM) (**Fig. S3**). The background methane in control reactors
205 resulted from carry-over substrates, once this was subtracted, the additional methane produced by *M.*
206 *barkeri* in poised reactors (3.1 ± 0.34 mM) could be solely credited to electricity. Moreover, the highest
207 rate of methane production was observed when current density profiles indicated the highest current
208 draw by *M. barkeri* (Fig. 3).

209 There are two possible scenarios for *M. barkeri* growing successfully at a cathode poised at -400 mV:

- 210 1. It may use low concentrations of H_2 generated electrochemically at the cathode, or
- 211 2. It retrieves electrons directly via an unknown mechanism

212 To determine abiotic electrochemical H_2 evolution we i) verified for H_2 accumulation over a month of
213 incubation and ii) verified the threshold for H_2 -evolution by linear sweep voltammetry at the beginning
214 and the end of the incubation. H_2 did not accumulate over a month of incubation in six independent
215 abiotic controls (**Fig. 4A**). Linear sweep voltammetry profiles indicated that in our media the threshold
216 for H_2 -evolution was below -700 mV (**Fig. 4B**). This was in agreement with previous studies

217 determining electrochemical H₂-evolution under physiological conditions on a graphite electrode, which
218 was below -400 mV due to high overpotentials (Batlle-Vilanova et al., 2014; Beese-Vasbender et al.,
219 2015; Cheng et al., 2009; Mitov et al., 2012).

220 On the other hand, in reactors inoculated with *M. barkeri*, the detected H₂ stabilized at 0.065 ± 0.02
221 mM, similar to concentrations observed for co-cultures of *M. barkeri* with (0.077 ± 0.03 mM) or
222 without conductive particles (0.076 ± 0.06 mM) and in pure culture (0.068 mM). This is supported by
223 previous research, which demonstrated H₂-cycling (H₂-production and H₂-uptake) in *M. barkeri*
224 (Kulkarni et al., 2009, 2018; Mand et al., 2018). The cellular evolved H₂ is well above the H₂-uptake
225 threshold for *M. barkeri* (296 nM - 376 nM) (Kral et al., 1998; Lovley, 1985) possibly because in these
226 cultures there is an alternative, competitive electron donor.

227 Secondly, if H₂ evolved electrochemically to concentrations under the detection limit (which was not
228 the case, see above), we anticipated that a sensitive hydrogenotrophic methanogen could effectively
229 reclaim low concentrations of electrochemical H₂, draw current and produce methane. To test this
230 hypothesis we used a highly effective H₂-utilizing methanogen – *M. formicicum*, which has a low H₂
231 uptake threshold of approximately 6 nM (Lovley, 1985). However, when *M. formicicum* was incubated
232 in electrochemical reactors, neither H₂, methane nor current draw was observed at – 400 mV (**Fig. 5**)
233 indicating that methanogenesis from H₂ could not occur at this potential. In addition, to ensure that the
234 growth of *M. formicicum* was unrestrained by the poised electrode, we carried control incubations at –
235 400 mV with extrinsic H₂ as substrate. *M. formicicum* was unaffected by a poised electrode since it
236 produced methane from the extrinsic H₂ in an electrochemical setup (**Fig. S4**).

237 As electrochemical H₂ was unlikely in our electrochemical setup, according to cumulative gas-detection
238 analyses, electrochemical tests, and tests with a highly effective H₂-utilizer, we confer that *M. barkeri* is
239 likely to retrieve electrons directly from the electrode.

240 *Methanosarcina horonobensis*

241 Except for *M. barkeri* and *M. harundinacea*, the distribution of extracellular electron uptake to other
242 species of the order Methanosarcinales has not been explored. *M. barkeri* and *M. harundinacea* species
243 have been isolated from and associated with anaerobic wastewater treatment (Bryant and Boone, 1987;

244 De Vrieze et al., 2012; Ma et al., 2006). We were interested to see if other environmentally relevant
245 *Methanosarcina* species had similar electron-uptake properties. We focused on *Methanosarcina*
246 *horonobensis* because of its provenience and consistent association with deep aquifers (Holmes et al.,
247 2018a; Shimizu et al., 2010).

248 *M. horonobensis* did establish successful syntrophic associations with *G. metallireducens* with or
249 without conductive particles as an electrical conduit (**Fig. 6**). Theoretically, *G. metallireducens* oxidizes
250 ethanol to acetate only if they could use the methanogen as an electron acceptor (Reaction 1). The
251 acetate is then further disproportionated by the acetoclastic methanogen to produce methane and CO₂
252 (Reaction 2 & 3). During DIET we expect the conversion of 1 mol ethanol to 1.5 mol methane
253 according to Reactions 1 to 3 (Fig. 1). As predicted, in the *G. metallireducens* – *M. horonobensis* co-
254 cultures, the syntroph oxidized 8.8 ± 0.4 mM ethanol providing the reducing equivalents (directly and
255 via acetate) to generate 13.1 ± 0.8 mM CH₄ by the methanogen. These co-cultures achieved
256 stoichiometric recoveries of 98.5 ± 3.3 %. Similar recoveries (109 ± 18.5 %) were also observed at the
257 addition of conductive particles. Single species controls with GAC showed that ethanol could not be
258 converted to methane by the methanogen or the syntroph alone (**Fig. 6C & S5**). However, similar to
259 previous reports (Zhang et al., 2018), *Geobacter* could partially convert ethanol to acetate using GAC as
260 insoluble electron acceptor (Fig. S5; Van Der Zee et al., 2003; Zhang et al., 2018), likely until it reaches
261 its maximum capacitance of 40 F/g (Zhang et al., 2009). Co-cultures of *G. metallireducens* and *M.*
262 *horonobensis* could not carry interspecies H₂ transfer because *G. metallireducens* is a strict respiratory
263 microorganism which cannot ferment ethanol to generate H₂ (Shrestha et al., 2013) and because *M.*
264 *horonobensis* is unable to use H₂ as electron donor for their metabolism (Shimizu et al., 2010).

265 Surprisingly, *M. horonobensis*, which could grow by DIET, was incapable of electromethanogenesis
266 (**Fig. 7**). Thus we compared the genomes of the two *Methanosarcina*, *M. horonobensis* and *M. barkeri*
267 to further explain why they were both capable of DIET, but showed dissimilar activities on cathodes at -
268 400mV.

269 The main difference between the genomes of *M. barkeri* and *M. horonobensis*, was related to their
270 energy metabolism (**Table 1**). *M. barkeri* utilizes an energy-converting hydrogenase (Ech) (Kulkarni et
271 al., 2018), which couples the reduction of protons with ferredoxin (Fdx⁻) to the production of a proton

272 motive force according to the reaction: $\text{Fdx}^- (\text{red}) + 2\text{H}^+ \rightarrow \text{Fdx} (\text{ox}) + \text{H}_2 + \Delta\mu\text{H}^+ / \Delta\mu\text{Na}^+$ (Thauer et
273 al., 2008). *M. horonobensis* does not have the Ech (Table 1). An alternative to Ech is the Na^+ -pumping
274 Rnf complex described biochemically in *M. acetivorans* (Schlegel et al., 2012; Suharti et al., 2014), and
275 predicted via genome mining in *M. thermophila* (Wang et al., 2011) and ANME-2 archaea (Wang et al.,
276 2014). Since we could not find any Ech in the genome of *M. horonobensis*, we screened for the genes
277 encoding an Rnf-complex. In *M. horonobensis*, we found all eight representative Rnf-genes (including
278 the cytochrome subunit and Rnf A to G; MSHOH_3554 to 3561), which showed 65-91% protein
279 identity to their *M. acetivorans* counterparts (MA_0658 to 0665).

280 Both Ech and Rnf contain Fe-S centers (Welte and Deppenmeier, 2014), however, the Rnf complex has
281 an accompanying *c*-type cytochrome (Suharti et al., 2014) possibly influencing the overall redox-
282 chemistry on the cell surface. We presume that differences in surface redox chemistry will impact how
283 different *Methanosarcina* interact with extracellular electron donors. Thus, electromethanogenesis at a
284 set potential of -400 mV is unlikely to match the redox requirements of each type of *Methanosarcina*.
285 On the other hand, in co-cultures, *Geobacter* may coordinate its cytochrome expression to match the
286 redox potential of the partner methanogen, who plays the role of a terminal electron acceptor. This is
287 supported by previous studies showing *Geobacter* modulates their cell-surface proteins to match the
288 electron acceptor provided (Ishii et al., 2018; Otero et al., 2018).

289 When contrasting the genomes of the two *Methanosarcina* species we also observed significant
290 differences regarding nitrogen fixation, mobile elements, and sensing/chemotaxis proteins (**Table 2**). As
291 such, compared to *M. horonobensis*, *M. barkeri* encodes for more N_2 -fixation proteins (86%).
292 Compared to *M. barkeri*, *M. horonobensis* encodes for more small-molecule-interaction proteins such
293 as redox-sensing and chemotaxis proteins (185%) and mobile elements than *M. barkeri* (16 fold
294 increase) (**Table 2**). The exact role of these proteins in extracellular electron uptake by these
295 *Methanosarcinas* is unknown and warrants further investigation.

296 Furthermore, to determine why *Methanosarcina* could do DIET, but not *Methanobacterium*, we
297 compared the genomes of the two *Methanosarcina* species with that of *M. formicicum* (**Table 2**). In
298 contrast to the *Methanobacterium*, both *Methanosarcina* species encode in their genomes three times
299 the amount of genes for electron transport proteins and circa 50% more genes for cell surface and

300 transport proteins (**Table 2**). Especially, outer surface S-layer proteins were only present in the two
301 *Methanosarcina* (Table 2). S-layer proteins were previously suggested to play a role in extracellular
302 electron transfer in *Methanosarcina* related ANME-2, which carry anaerobic methane oxidation
303 syntrophically (McGlynn, 2017; McGlynn et al., 2015; Timmers et al., 2017). Future gene-expression
304 and deletion studies could shed light on the possible role of S-layer proteins in DIET-interactions.

305 **Conclusion**

306 Three methanogens were investigated for their ability to do extracellular electron uptake from (1) a
307 cathode at -400 mV, (2) directly from an electrogenic-DIET partner or (3) from a DIET-partner, but
308 mediated by conductive particles. Only *M. barkeri* was able to carry out all three forms of extracellular
309 electron uptake, making this the first observation of a *Methanosarcina* in pure culture performing
310 electromethanogenesis. The conditions in our abiotic electrochemical controls did not lead to H₂-
311 evolution at -400mV, according to electrochemical and analytical tests. Therefore, under these
312 conditions, it was impossible to sustain a methanogen with high H₂-affinity, like *M. formicicum*.
313 Besides *M. formicicum* was incapable to retrieve electrons directly from the electrode or from a DIET
314 partner (direct or via conductive particles). In this study, we also demonstrated that another
315 *Methanosarcina*, *M. hornobensis* performed DIET with *Geobacter* (direct or via conductive particles).
316 However, surprisingly, *M. hornobensis* was incapable of electromethanogenesis. We screened the
317 genomes of the two *Methanosarcina* and identified differences (e.g. energy metabolism), which could
318 lead to phenotypic variability and thus contrasting electromethanogenesis-ability. Compared to *M.*
319 *barkeri*, *M. hornobensis* is a better candidate for understanding electron uptake from a DIET
320 syntrophic partner. This is because unlike *M. barkeri*, *M. hornobensis* does not utilize H₂, and it grows
321 as single cells on freshwater media, which is ideal for genetic studies.

322 **Acknowledgments**

323 The Innovationsfond grant number 4106-00017 funded this work. We would like to thank Lasse Ørum
324 Smidt and Heidi Grøn Jensen for lab assistance.

325 **Author contribution**

326 MY and A-ER conceived the study with support from BT and LO. MY performed all experiments with
327 support from OS. MY analyzed the data with support from A-ER. MY wrote the manuscript with help
328 from A-ER. All authors (MY, A-ER, BT, OS and LO) contributed to drafting and editing the
329 manuscript.

330 **References**

- 331 Aklujkar, M., Krushkal, J., Dibartolo, G., Lapidus, A., Land, M. L., and Lovley, D. R. (2009). The
332 genome sequence of *Geobacter metallireducens*: Features of metabolism, physiology and
333 regulation common and dissimilar to *Geobacter sulfurreducens*. *BMC Microbiol.* 9, 1–22.
334 doi:10.1186/1471-2180-9-109.
- 335 Batlle-Vilanova, P., Puig, S., Gonzalez-Olmos, R., Vilajeliu-Pons, A., Bañeras, L., Balaguer, M. D., et
336 al. (2014). Assessment of biotic and abiotic graphite cathodes for hydrogen production in
337 microbial electrolysis cells. *Int. J. Hydrogen Energy* 39, 1297–1305.
338 doi:10.1016/j.ijhydene.2013.11.017.
- 339 Beese-Vasbender, P. F., Grote, J.-P., Garrelfs, J., Stratmann, M., and Mayrhofer, K. J. J. (2015).
340 Selective microbial electrosynthesis of methane by a pure culture of a marine lithoautotrophic
341 archaeon. *Bioelectrochemistry* 102, 50–55. doi:10.1016/j.bioelechem.2014.11.004.
- 342 Bryant, M. P., and Boone, D. R. (1987). Emended Description of Strain MST(DSM 800T), the Type
343 Strain of *Methanosarcina barkeri*. *Int. J. Syst. Bacteriol.* 37, 169–170. doi:10.1099/00207713-37-2-
344 169.
- 345 Buckel, W., and Thauer, R. K. (2013). Energy conservation via electron bifurcating ferredoxin
346 reduction and proton/Na⁺ translocating ferredoxin oxidation. *Biochim. Biophys. Acta - Bioenerg.*
347 1827, 94–113. doi:10.1016/j.bbabi.2012.07.002.
- 348 Buckel, W., and Thauer, R. K. (2018). Flavin-based electron bifurcation, ferredoxin, flavodoxin, and
349 anaerobic respiration with protons (Ech) or NAD⁺(Rnf) as electron acceptors: A historical review.
350 *Front. Microbiol.* 9. doi:10.3389/fmicb.2018.00401.

- 351 Chen, S., Rotaru, A.-E., Liu, F., Philips, J., Woodard, T. L., Nevin, K. P., et al. (2014a). Carbon cloth
352 stimulates direct interspecies electron transfer in syntrophic co-cultures. *Bioresour. Technol.* 173,
353 82–86. doi:10.1016/j.biortech.2014.09.009.
- 354 Chen, S., Rotaru, A.-E., Shrestha, P. M., Malvankar, N. S., Liu, F., Fan, W., et al. (2014b). Promoting
355 Interspecies Electron Transfer with Biochar. *Sci. Rep.* 4, 1–7. doi:10.1038/srep05019.
- 356 Cheng, S., Xing, D., Call, D. F., and Logan, B. E. (2009). Direct biological conversion of electrical
357 current into methane by electromethanogenesis. *Environ. Sci. Technol.* 43, 3953–3958.
358 doi:10.1021/es803531g.
- 359 Cord-Ruwisch, R., Lovley, D. R., & Schink, B. (1998). Growth of *Geobacter sulfurreducens* with
360 acetate in syntrophic cooperation with hydrogen-oxidizing anaerobic partners. *Appl. Environ.*
361 *Microbiol.*, 64(6), 2232–2236.
- 362 Dang, Y., Holmes, D. E., Zhao, Z., Woodard, T. L., Zhang, Y., Sun, D., et al. (2016). Enhancing
363 anaerobic digestion of complex organic waste with carbon-based conductive materials. *Bioresour.*
364 *Technol.* 220, 516–522. doi:10.1016/j.biortech.2016.08.114.
- 365 De Vrieze, J., Hennebel, T., Boon, N., and Verstraete, W. (2012). Methanosarcina: the rediscovered
366 methanogen for heavy duty biomethanation. *Bioresour. Technol.* 112, 1–9.
367 doi:10.1016/j.biortech.2012.02.079.
- 368 Holmes, D. E., Orelana, R., Giloteaux, L., Wang, L.-Y., Shrestha, P. M., Williams, K., et al. (2018a).
369 Potential for Methanosarcina to Contribute to Uranium Reduction during Acetate-Promoted
370 Groundwater Bioremediation. *Microb. Ecol.*, 1–8. doi:10.1007/s00248-018-1165-5.
- 371 Holmes, D. E., Rotaru, A.-E., Ueki, T., Shrestha, P. M., Ferry, J. G., and Lovley, D. R. (2018b).
372 Electron and Proton Flux for Carbon Dioxide Reduction in *Methanosarcina barkeri* During Direct
373 Interspecies Electron Transfer. *Front. Microbiol.* 9, 3109. doi:10.3389/fmicb.2018.03109.
- 374 Holmes, D. E., Shrestha, P. M., Walker, D. J. F., Dang, Y., Nevin, K. P., Woodard, T. L., et al. (2017a).
375 Metatranscriptomic Evidence for Direct Interspecies Electron Transfer Between *Geobacter* and

- 376 Methanotherix Species in Methanogenic Rice Paddy Soils. *Appl. Environ. Microbiol.*, AEM.00223-
377 17. doi:10.1128/AEM.00223-17.
- 378 Holmes, D. E., Shrestha, P. M., Walker, D. J. F., Dang, Y., Nevin, K. P., Woodard, T. L., et al. (2017b).
379 Metatranscriptomic Evidence for Direct Interspecies Electron Transfer between *Geobacter* and
380 Methanotherix Species in Methanogenic Rice Paddy Soils. *Appl. Environ. Microbiol.* 83, e00223-
381 17. doi:10.1128/AEM.00223-17.
- 382 Ishii, S., Suzuki, S., Tenney, A., Nealson, K. H., and Bretschger, O. (2018). Comparative
383 metatranscriptomics reveals extracellular electron transfer pathways conferring microbial
384 adaptivity to surface redox potential changes. *ISME J.* doi:10.1038/s41396-018-0238-2.
- 385 Kral, T. A., Brink, K. M., Miller, S. L., and McKay, C. P. (1998). Hydrogen consumptions by
386 methanogens on the early earth. *Orig. Life Evol. Biosph.* 28, 311–319. doi:Doi
387 10.1023/A:1006552412928.
- 388 Kulkarni, G., Kridelbaugh, D. M., Guss, A. M., and Metcalf, W. W. (2009). Hydrogen is a preferred
389 intermediate in the energy-conserving electron transport chain of *Methanosarcina barkeri*. *Proc.*
390 *Natl. Acad. Sci. U. S. A.* 106, 15915–20. doi:10.1073/pnas.0905914106.
- 391 Kulkarni, G., Mand, T. D., and Metcalf, W. W. (2018). Energy Conservation via Hydrogen Cycling in
392 the Methanogenic Archaeon *Methanosarcina barkeri*. *MBio* 9, 1–10. doi:10.1128/mBio.01256-18.
- 393 Lee, J. Y., Lee, S. H., and Park, H. D. (2016). Enrichment of specific electro-active microorganisms and
394 enhancement of methane production by adding granular activated carbon in anaerobic reactors.
395 *Bioresour. Technol.* 205, 205–212. doi:10.1016/j.biortech.2016.01.054.
- 396 Lin, Q., Fang, X., Ho, A., Li, J., Yan, X., Tu, B., et al. (2017). Different substrate regimes determine
397 transcriptional profiles and gene co-expression in *Methanosarcina barkeri* (DSM 800). *Appl.*
398 *Microbiol. Biotechnol.*, 1–14. doi:10.1007/s00253-017-8457-4.
- 399 Liu, F., Rotaru, A.-E., Shrestha, P. M., Malvankar, N. S., Nevin, K. P., and Lovley, D. R. (2012).
400 Promoting direct interspecies electron transfer with activated carbon. *Energy Environ. Sci.* 5, 8982.

401 doi:10.1039/c2ee22459c.

402 Lovley, D. R. (1985). Minimum threshold for hydrogen metabolism in methanogenic bacteria. *Appl.*
403 *Environ. Microbiol.* 49, 1530–1.

404 Lovley, D. R. (2017). Syntrophy Goes Electric: Direct Interspecies Electron Transfer. *Annu. Rev.*
405 *Microbiol.* 71, annurev-micro-030117-020420. doi:10.1146/annurev-micro-030117-020420.

406 Lovley, D. R., Giovannoni, S. J., White, D. C., Champine, J. E., Phillips, E. J. P., Gorby, Y. A., et al.
407 (1993). *Geobacter metallireducens* gen. nov. sp. nov., a microorganism capable of coupling the
408 complete oxidation of organic compounds to the reduction of iron and other metals. *Arch*
409 *Microbiol* 159, 336–344.

410 Ma, K., Liu, X., and Dong, X. (2006). *Methanosaeta harundinacea* sp. nov., a novel acetate-scavenging
411 methanogen isolated from a UASB reactor. *Int. J. Syst. Evol. Microbiol.* 56, 127–131.
412 doi:10.1099/ijss.0.63887-0.

413 Mand, T. D., Kulkarni, G., and Metcalf, W. W. (2018). Genetic, Biochemical, and Molecular
414 Characterization of *Methanosarcina barkeri* Mutants Lacking Three Distinct Classes of
415 Hydrogenase. *J. Bacteriol.* 200, e00342-18. doi:10.1128/JB.00342-18.

416 McGlynn, S. E. (2017). Energy Metabolism during Anaerobic Methane Oxidation in ANME Archaea.
417 *Microbes Environ.* 32, 5–13. doi:10.1264/jsme2.ME16166.

418 McGlynn, S. E., Chadwick, G. L., Kempes, C. P., and Orphan, V. J. (2015). Single cell activity reveals
419 direct electron transfer in methanotrophic consortia. *Nature* 526, 531–535.
420 doi:10.1038/nature15512.

421 Meuer, J., Kuettner, H. C., Zhang, J. K., Hedderich, R., and Metcalf, W. W. (2002). Genetic analysis of
422 the archaeon *Methanosarcina barkeri* Fusaro reveals a central role for Ech hydrogenase and
423 ferredoxin in methanogenesis and carbon fixation. *Proc. Natl. Acad. Sci.* 99, 5632–5637.
424 doi:10.1073/pnas.072615499.

425 Mitov, M., Chorbadzhiyska, E., Rashkov, R., and Hubenova, Y. (2012). Novel nanostructured

- 426 electrocatalysts for hydrogen evolution reaction in neutral and weak acidic solutions. *Int. J.*
427 *Hydrogen Energy* 37, 16522–16526. doi:10.1016/J.IJHYDENE.2012.02.102.
- 428 Morris, B. E. L., Henneberger, R., Huber, H., and Moissl-Eichinger, C. (2013). Microbial syntrophy:
429 interaction for the common good. *FEMS Microbiol. Rev.* 37, 384–406. doi:10.1111/1574-
430 6976.12019.
- 431 Otero, F. J., Chan, C. H., and Bond, D. R. (2018). Identification of Different Putative Outer Membrane
432 Electron Conduits Necessary for Fe(III) Citrate, Fe(III) Oxide, Mn(IV) Oxide, or Electrode
433 Reduction by *Geobacter sulfurreducens* Downloaded from. *J. Bacteriol.* 200, 347–365.
434 doi:10.1128/JB.00347-18.
- 435 Rotaru, A.-E., Calabrese, F., Stryhanyuk, H., Musat, F., Shrestha, P. M., Weber, H. S., et al. (2018a).
436 Conductive Particles Enable Syntrophic Acetate Oxidation between *Geobacter* and
437 *Methanosarcina* from Coastal Sediments. *MBio* 9, 1–14. doi:10.1128/mBio.00226-18.
- 438 Rotaru, A.-E., Posth, N. R., Miracle, M. R., Vicente, E., Cox, R. P., Thompson, J., et al. (2018b).
439 Interspecies interactions mediated by conductive minerals in the sediments of the ferruginous Lake
440 La Cruz, Spain. *Limnetica*, 1–30.
- 441 Rotaru, A.-E., Shrestha, P. M., Liu, F., Markovaite, B., Chen, S., Nevin, K. P., et al. (2014a). Direct
442 Interspecies Electron Transfer between *Geobacter metallireducens* and *Methanosarcina barkeri*.
443 *Appl. Environ. Microbiol.* 80, 4599–4605. doi:10.1128/AEM.00895-14.
- 444 Rotaru, A.-E., Shrestha, P. M., Liu, F., Shrestha, M., Shrestha, D., Embree, M., et al. (2014b). A new
445 model for electron flow during anaerobic digestion: direct interspecies electron transfer to
446 *Methanosaeta* for the reduction of carbon dioxide to methane. *Energy Environ. Sci.* 7, 408–415.
447 doi:10.1039/C3EE42189A.
- 448 Rotaru, A.-E., Woodard, T. L., Nevin, K. P., and Lovley, D. R. (2015). Link between capacity for
449 current production and syntrophic growth in *Geobacter* species. *Front. Microbiol.* 6, 1–8.
450 doi:10.3389/fmicb.2015.00744.

- 451 Salvador, A. F., Martins, G., Melle-Franco, M., Serpa, R., Stams, A. J. M., Cavaleiro, A. J., et al.
452 (2017). Carbon nanotubes accelerate methane production in pure cultures of methanogens and in a
453 syntrophic coculture. *Environ. Microbiol.* 19, 2727–2739. doi:10.1111/1462-2920.13774.
- 454 Schlegel, K., Welte, C., Deppenmeier, U., and Müller, V. (2012). Electron transport during acetoclastic
455 methanogenesis by *Methanosarcina acetivorans* involves a sodium-translocating Rnf complex.
456 *FEBS J.* 279, 4444–4452. doi:10.1111/febs.12031.
- 457 Seiler, M., Mehrle, A., Poustka, A., and Wiemann, S. (2006). The 3of5 web application for complex
458 and comprehensive pattern matching in protein sequences. *BMC Bioinformatics* 7, 1–12.
459 doi:10.1186/1471-2105-7-144.
- 460 Shimizu, S., Upadhye, R., Ishijima, Y., and Naganuma, T. (2010). *Methanosarcina horonobensis* sp.
461 nov., a methanogenic archaeon isolated from a deep subsurface Miocene formation. *Int. J. Syst.*
462 *Evol. Microbiol.* 61, 2503–2507. doi:10.1099/ijs.0.028548-0.
- 463 Shrestha, P. M., and Rotaru, A.-E. (2014). Plugging in or going wireless: strategies for interspecies
464 electron transfer. *Front. Microbiol.* 5, 1–8. doi:10.3389/fmicb.2014.00237.
- 465 Shrestha, P. M., Rotaru, A.-E., Aklujkar, M., Liu, F., Shrestha, M., Summers, Z. M., et al. (2013).
466 Syntrophic growth with direct interspecies electron transfer as the primary mechanism for energy
467 exchange. *Environ. Microbiol. Rep.* 5, 904–910. doi:10.1111/1758-2229.12093.
- 468 Smith, T. J., and Stevenson, K. J. (2007). “Reference electrodes,” in *Handbook of Electrochemistry*
469 (Elsevier B.V.), 73–110. doi:10.1016/B978-0-444-51958-0.50005-7.
- 470 Stams, A. J. M., and Plugge, C. M. (2009). Electron transfer in syntrophic communities of anaerobic
471 bacteria and archaea. *Nat. Rev. Microbiol.* 7, 568–577. doi:10.1038/nrmicro2166.
- 472 Suharti, S., Wang, M., De Vries, S., and Ferry, J. G. (2014). Characterization of the RnfB and RnfG
473 subunits of the Rnf complex from the archaeon *Methanosarcina acetivorans*. *PLoS One* 9, 1–10.
474 doi:10.1371/journal.pone.0097966.
- 475 Thauer, R. K., Kaster, A.-K., Seedorf, H., Buckel, W., and Hedderich, R. (2008). Methanogenic

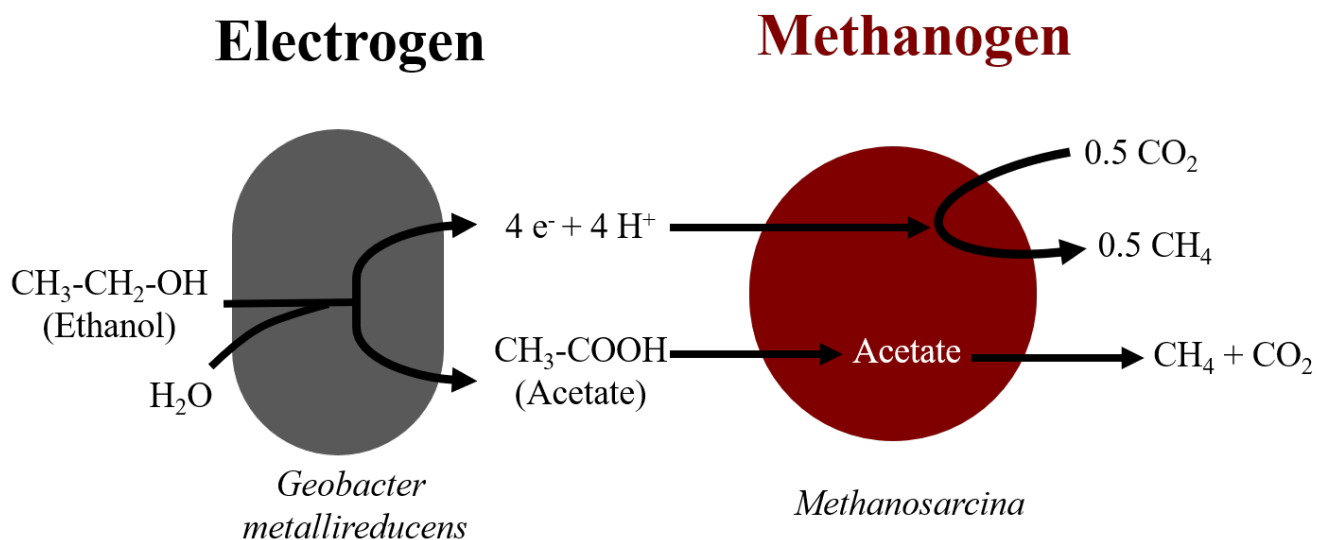
- 476 archaea: ecologically relevant differences in energy conservation. *Nat. Rev. Microbiol.* 6, 579–591.
477 doi:10.1038/nrmicro1931.
- 478 Timmers, P. H. A., Welte, C. U., Koehorst, J. J., Plugge, C. M., Jetten, M. S. M., and Stams, A. J. M.
479 (2017). Reverse Methanogenesis and Respiration in Methanotrophic Archaea. *Archaea* 2017.
480 doi:10.1155/2017/1654237.
- 481 Van Der Zee, F. P., Bisschops, I. A. E., Lettinga, G., & Field, J. A. (2003). Activated carbon as an
482 electron acceptor and redox mediator during the anaerobic biotransformation of azo dyes. *Environ.*
483 *Sci. Technol.*, 37(2), 402–408. <https://doi.org/10.1021/es025885o>
- 484 Wang, F. P., Zhang, Y., Chen, Y., He, Y., Qi, J., Hinrichs, K.-U., et al. (2014). Methanotrophic archaea
485 possessing diverging methane-oxidizing and electron-Transporting pathways. *ISME J.* 8, 1069–
486 1078. doi:10.1038/ismej.2013.212.
- 487 Wang, M., Tomb, J.-F., and Ferry, J. G. (2011). Electron transport in acetate-grown *Methanosarcina*
488 *acetivorans*. *BMC Microbiol.* 11. doi:10.1186/1471-2180-11-165.
- 489 Wang, O., Zheng, S., Wang, B., Wang, W., and Liu, F. (2018). Necessity of electrically conductive pili
490 for methanogenesis with magnetite stimulation. *PeerJ* 6, e4541. doi:10.7717/peerj.4541.
- 491 Welte, C. U., and Deppenmeier, U. (2014). Bioenergetics and anaerobic respiratory chains of
492 acetoclastic methanogens. *Biochim. Biophys. Acta - Bioenerg.* 1837, 1130–1147.
493 doi:10.1016/j.bbabi.2013.12.002.
- 494 Ye, Q., Zhang, Z., Huang, Y., Fang, T., Cui, Q., He, C., et al. (2018). Enhancing electron transfer by
495 magnetite during phenanthrene anaerobic methanogenic degradation. *Int. Biodeterior. Biodegrad.*,
496 0–1. doi:10.1016/j.ibiod.2018.01.012.
- 497 Zhang, L., Zhang, J., and Loh, K. C. (2018). Activated carbon enhanced anaerobic digestion of food
498 waste – Laboratory-scale and Pilot-scale operation. *Waste Manag.* 75, 270–279.
499 doi:10.1016/j.wasman.2018.02.020.
- 500 Zhang, P., Zheng, S., Liu, J., Wang, B., Liu, F., & Feng, Y. (2018). Surface properties of activated

- 501 sludge-derived biochar determine the facilitating effects on *Geobacter* co-cultures. *Water Res.*,
502 142, 441–451. <https://doi.org/10.1016/j.watres.2018.05.058>
- 503 Zhang, Y., Feng, H., Wu, X., Wang, L., Zhang, A., Xia, T., ... Zhang, L. (2009). Progress of
504 electrochemical capacitor electrode materials: A review. *Int. J. Hydrogen Energy*, 34(11), 4889–
505 4899. <https://doi.org/10.1016/j.ijhydene.2009.04.005>
- 506 Zheng, S., Zhang, H., Li, Y., Zhang, H., Wang, O., Zhang, J., et al. (2015). Co-occurrence of
507 *Methanosarcina mazei* and *Geobacteraceae* in an iron (III)-reducing enrichment culture. *Front.*
508 *Microbiol.* 6, 1–12. doi:10.3389/fmicb.2015.00941.
- 509 Zhuang, L., Tang, J., Wang, Y., Hu, M., and Zhou, S. (2015). Conductive iron oxide minerals accelerate
510 syntrophic cooperation in methanogenic benzoate degradation. *J. Hazard. Mater.* 293, 37–45.
511 doi:10.1016/j.jhazmat.2015.03.039.

512

513 **Figures**

514 (Fig. 1) Diagram of electron flow during DIET interactions between *Geobacter metallireducens* and
515 *Methanosarcina*-species provided with ethanol as sole electron donor.



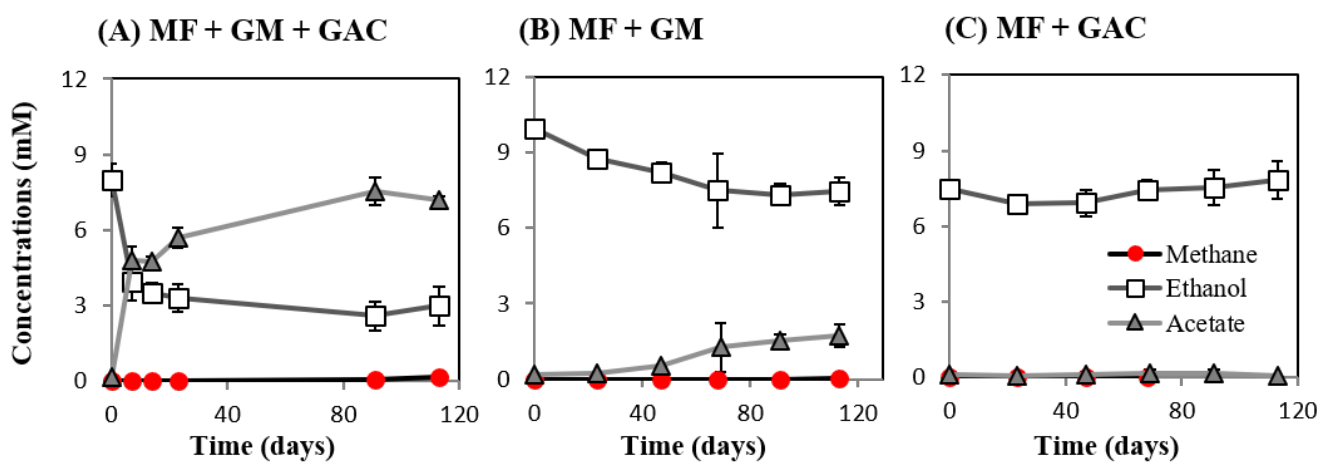
Total reaction: 1 mol Ethanol \longrightarrow 1.5 mol CH_4 + 0.5 mol CO_2

516

517

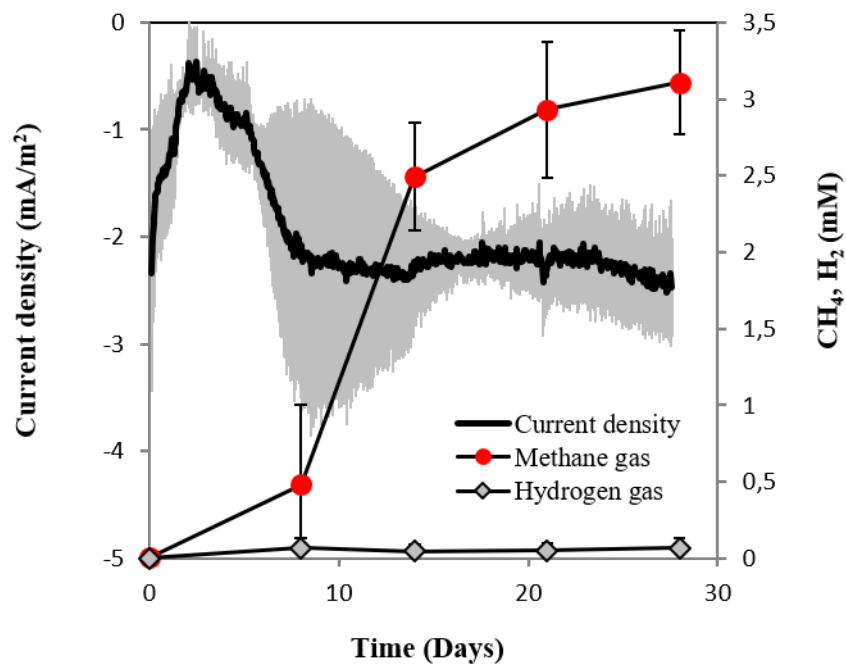
518

519 (Fig. 2) Co-cultures experiments with *M. formicicum* and *G. metallireducens* (n=3). *M. formicicum* did
520 not produce methane when incubated with *G. metallireducens* in the presence (A) or absence of GAC
521 (B). Alone, *M. formicicum* could not utilize ethanol or produce methane in the presence of GAC. MF -
522 *Methanobacterium formicicum*, GM - *Geobacter metallireducens*, GAC - granular activated carbon.



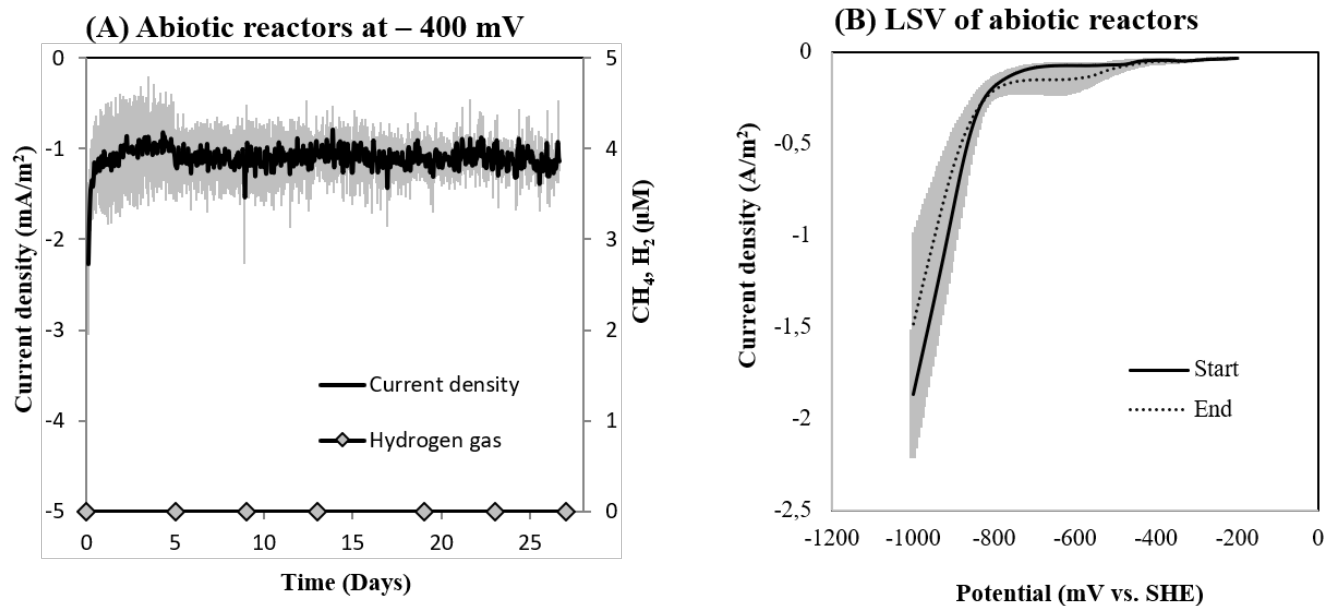
523

524 (Fig. 3) Current consumption and gas production in triplicate *M. barkeri* cultures provided with a poised
525 cathode at -400 mV (vs. SHE) as sole electron donor.



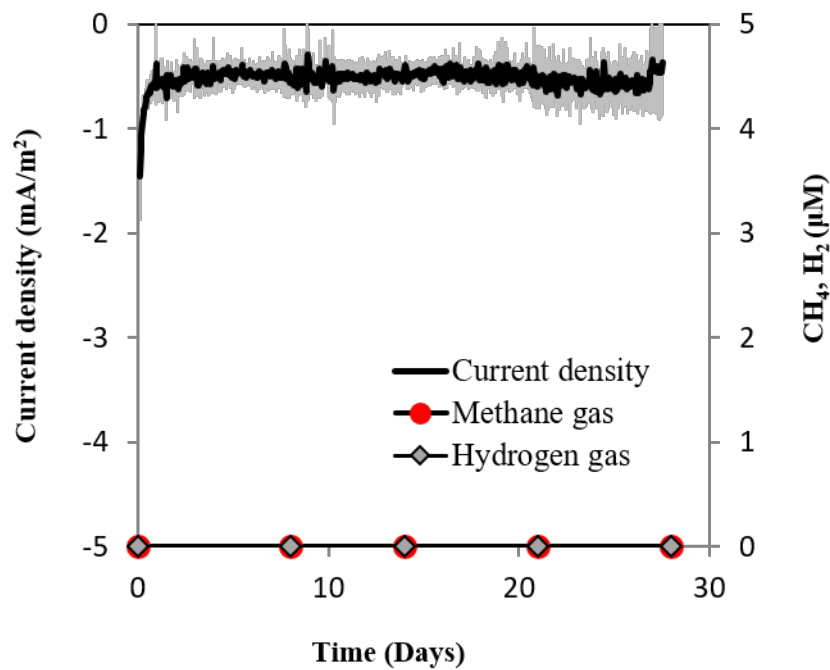
526

527 (Fig. 4) (A) Current consumption and gas production in four abiotic reactors at -400 mV (vs. SHE) and
528 (B) Linear Sweep Voltammetry (LSV) of abiotic reactors at the start and end of the experiment (n=3).



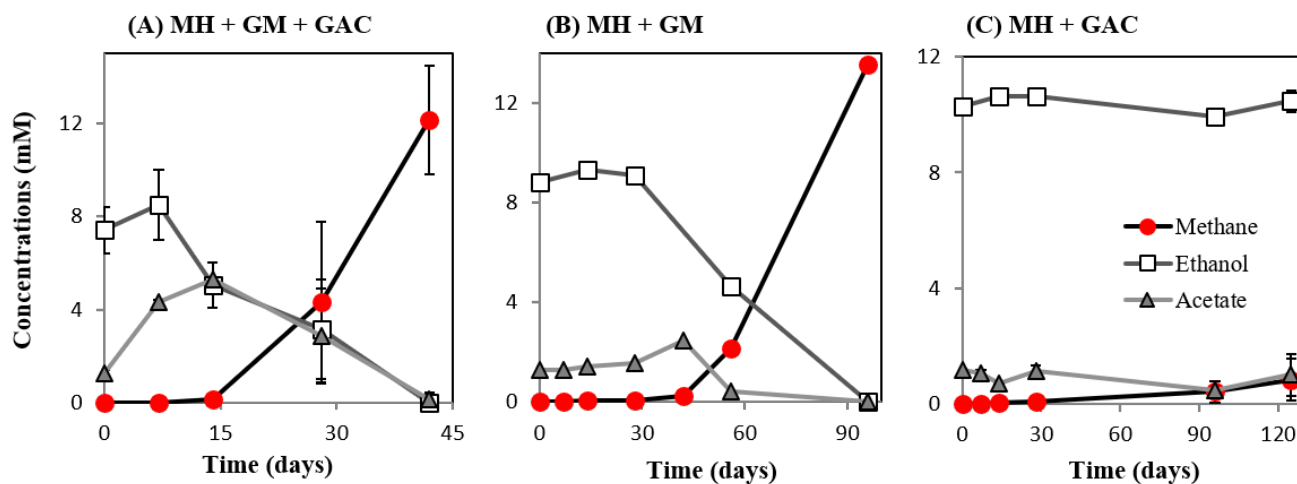
529
530

531 (Fig. 5) Current consumption and gas production in triplicate *M. formicicum* cultures provided with a
532 cathode poised at - 400 mV (vs. SHE) as sole electron donor.



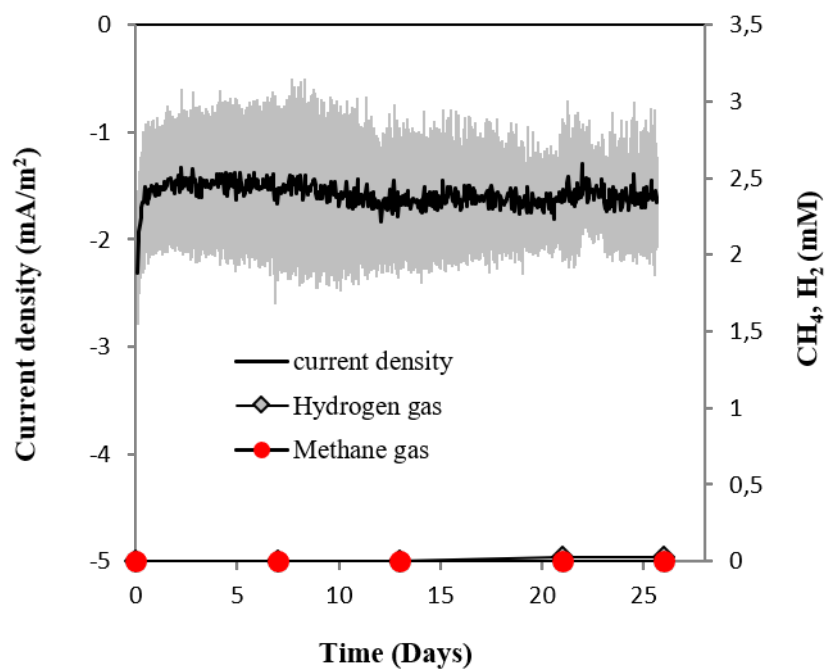
533

534 (Fig. 6) Co-culture experiments with *M. horonobensis* and *G. metallireducens*. *M. horonobensis*
535 established successful co-cultures with *G. metallireducens* as apparent from ethanol utilization and
536 methane production in the presence (A, n=3) or absence of GAC (B, n=1; see replication in Fig. S6).
537 Alone, *M. horonobensis* could not utilize ethanol or produce methane in the presence of GAC (C, n=3).
538 MH - *Methanosarcina horonobensis*, GM - *Geobacter metallireducens*, GAC - granular activated
539 carbon.



540

541 (Fig. 7) Current consumption and gas production in cultures of *M. horonobensis* (n=3) provided with a
542 cathode poised at - 400 mV (vs. SHE) as sole electron donor.



543

544

545 **Tables**

546 (Table 1) Relevant genotypic differences between the methanogens tested during this study

Species	Energy conservation	S-layer proteins	Predicted c-type cytochromes (CxxCH motif proteins)	Other cytochromes	Predicted Ferredoxins	Predicted thioredoxins
<i>Methanosarcina barkeri</i> MS	Ech-hydrogenase	8	20 (0/1 multiheme*)	3 (cyt b)	4	10
<i>Methanosarcina horonobensis</i> HB-1	Rnf-complex	9	30 (3 multiheme)	3 (cyt b)	6	8
<i>Methanobacterium formicicum</i> DSM1535	EhaA/EhbA hydrogenase	None	16 (None)	None	4	2

*The predicted multiheme cytochrome in *M. barkeri* strain MS had one standard CxxCH and one CxCH motif.

547
548

549 (Table 2) Genomic comparison of three methanogens based on TIGR family protein categories.

TIGRfam Categories	No. of genes associated within a TIGR family		
	<i>Methanosarcina horonobensis</i>	<i>Methanosarcina barkeri</i>	<i>Methanobacterium formicicum</i>
Fatty acid and phospholipid metabolism	3	4	3
Transcription	13	12	13
Central intermediary metabolism	21	27	21
- Nitrogen fixation	7	13	7
Cell processes	26	18	22
Cell envelope	28	27	14
- Surface structures (S-layer)	9	8	0
Purines, pyrimidines, nucleosides, and nucleotides	33	33	33
Mobile and extrachromosomal element functions	39	2	2
- Transposons	32	2	0
DNA metabolism	43	38	27
Protein fate	48	44	33
Amino acid biosynthesis	56	57	57
Biosynthesis of cofactors, prosthetic groups, and carriers	60	61	65
- Heme, prothyrin, cobalamin	22	25	19
Regulatory functions	84	33	51
- Small molecule interactions	77	27	40
Protein synthesis	87	89	75
Energy metabolism	95	86	64
- Electron transport proteins	21	17	7
Transport and binding proteins	97	85	63
- Iron carrying compounds	51	44	29
- Aminoacids and amines	17	12	0
Unknown and hypothetical	119	78	92

550